RSC Advances

PAPER

View Article Online
View Journal | View Issue

Check for updates

Cite this: *RSC Adv.*, 2026, **16**, 26948

Maleic acid assisted facile plasmonic chip for assessment of adulterants in cattle milk

Upama Das,[a] Tonmoy Dhar,[a] Rajib Biswas *[a] and Nirmal Mazumder*[b]

Adulteration in cattle milk is a pervasive issue, where melamine is added to milk due to its high nitrogen content, which ultimately falsely elevates the perceived protein levels of milk. However, its consumption possesses a significant threat, because it can cause severe health hazards. Conventional detection methods are often very expensive and also lack selectivity, and sensitivity towards detection of toxic adulterants. This study addresses these limitations by fabricating a highly selective maleic acid-functionalized silver nanoparticles (MA-AgNPs) based plasmonic nanofilm for highly accurate detection of milk adulterant melamine. At first, chemical reduction method was used to synthesize the AgNP swhich was later functionalized with maleic acid. The functionalized NPs were uniformly coated onto a glass slide to create localized surface plasmon resonance (LSPR) chip. The plasmonic activity of the NPs along with its selective interaction towards melamine resulted in significant shift in plasmonic peak position, enabling melamine detection below the permissible limit. To determine the optical and physical properties of the synthesized AgNPs, UV-vis spectrophotometer, X-ray diffractometer (XRD), Field Emission Scanning Electron Microscope (FESEM), Atomic Force Microscope (AFM), and Transmission Electron Microscope (TEM) studies were conducted. Validation of the milk samples spiked with melamine was performed utilizing the High-Performance Liquid Chromatography (HPLC) method. The developed LSPR-based platform offered a sustainable and inexpensive solution for detecting milk adulterant melamine, with high sensitivity, selectivity and lower detection limit.

Received 4th August 2025
Accepted 22nd April 2026

DOI: 10.1039/d5ra05664k

rsc.li/rsc-advances

Open Access Article. Published on 19 May 2026. Downloaded on 5/22/2026 8:11:50 PM.
This article is licensed under a Creative Commons Attribution-NonCommercial 3.0 Unported Licence.

1 Introduction

Plasmonic nanostructures (NSs) display extraordinary optical properties that can be tuned by altering several factors such as shape, size, and composition, as well as the external surrounding medium.[1] Their unique characteristics enable their use in wide range of applications across various domains, such as detection of heavy metals,[2] pesticides,[3] food adulterants,[4] various toxic chemicals[5] and contaminants. Among various reported cases of food adulteration, milk stands out as one of the most commonly adulterated food item consumed worldwide. Various substances are added to milk for a wide variety of reasons, such as extending its shelf life, or falsifying its net protein content, *etc.*[6] Melamine, for instance, is often added as a rich nitrogen source to falsify the net content of protein in milk.[4,6] However, ingestion of melamine, poses severe health risks, as reported during the milk scandal which has occurred in China in the year 2008.[7,8]

To prevent such instances of milk adulteration strict regulatory limits are imposed on presence of milk adulterant melamine by the government regulatory bodies worldwide. For example, the Food Safety and Standards Authority of India (FSSAI) recommend a maximum permissible limit for melamine concentration of 2.5 ppm for adults and less than 1 ppm for infants.[9] Similarly, the Food and Drug Administration (U.S. FDA) and the Ministry of Food and Drug Safety in South Korea have also established their own guidelines to safeguard public health.[9,10] To curb this issue, regular monitoring of such adulterants is highly recommended, which is only possible with fabrication of sensitive and highly reliable detection methods. Plasmonic-based sensing platforms have the potential to address the regulatory requirements by offering wide range of advantages such as portability, ease of use, and inexpensiveness.

Conventional analytical methods like HPLC[11] and gas chromatography/mass spectrometry (GC/MS)[12] are typically utilised to sense milk adulterants. However, the techniques are sophisticated and require the involvement of trained personnel, making routine monitoring of milk adulterants highly challenging. Alternative approaches, includes development of aptamer-based sensors,[13] quantum dots[14] and colorimetric sensors[4,6,15–19] have also been studied for detection of melamine. While, in majority of the techniques NPs in colloidal form is used for sensing, which is quite simple and rapid method; however, such methods primarily help in qualitative analysis.

[a]*Applied Optics and Photonics Research Laboratory, Department of Physics, Tezpur University, Tezpur-784028, Assam, India. E-mail: rajib@tezu.ernet.in*

[b]*Department of Biophysics, Manipal School of Life Sciences, Manipal Academy of Higher Education, Manipal, India. E-mail: nirmal.mazumder@manipal.edu*

© 2026 The Author(s). Published by the Royal Society of Chemistry

Open Access Article. Published on 19 May 2026. Downloaded on 5/22/2026 8:11:50 PM.
This article is licensed under a Creative Commons Attribution-NonCommercial 3.0 Unported Licence.

This limits their usefulness for obtaining precise, reproducible, and quantitative outputs. Moreover, AgNPs in liquid media are highly unstable and aggregate more easily over time. Such aggregation reduces the stability the NPs and thereby, hinders the reproducibility of the detection system. However, Surface Enhanced Raman Scattering (SERS) technique[20] and electrochemical sensors[21] are also found to be highly useful, but they require significant sample preparation time and sophisticated analysis protocols, limiting their use in practical applications. To solve these challenges, the fabrication of a user-friendly and rapid sensing method for detection of melamine is highly necessary. In this context, plasmonic NSs offers cost-effective, highly reliable solution for fabrication of portable, sensitive and rapid detection device for sensing of milk adulterants.[22,23] By utilising the interaction mechanism between melamine and the plasmonic NSs, it is possible to detect melamine with minimal steps of sample pretreatment.[4,6]

To solve this problem and address the gap, this study proposes a new and highly efficient method for detecting melamine in raw milk, which offers exceptional simplicity and eliminates the requirement for any complex NP fabrication technique or extensive sample preparation. The reported approach involves fabrication of plasmonic NPs using a conventional borohydride reduction method, which is followed by their functionalization with maleic acid. These surface-functionalized NPs were coated onto a microscopic glass slide. This fabricated substrate acts as a highly selective LSPR chip capable of detecting minute changes in the refractive index of the medium surrounding the NPs induced by the presence of melamine in milk. The size of the chip is so small that it can be compared with the dimension of a coin (Fig. 1).

In contrast to colorimetric sensing, immobilizing AgNPs on a glass substrate to form a plasmonic nanofilm offers several advantages such as it prohibits NPs aggregation, the LSPR signal can be quantitatively monitored with high sensitivity and reproducibility, and the solid substrate configuration allows for controlled interaction with analytes, enabling consistent and repeatable results. Therefore, the chip-based plasmonic sensing approach used in this work provides a more reliable, quantitative, and reproducible detection platform compared to conventional colorimetric sensing using colloidal NPs. The synthesis route was deliberately optimized to improve NP selectivity toward the melamine molecule. The fabricated sensor delivered a straightforward, stable, and affordable solution for detecting melamine levels in milk. Here, maleic acid molecules play a crucial role as functional linkers, enabling selective melamine binding. This interaction produces a measurable plasmonic shift, which can be calibrated for accurate quantitative analysis.

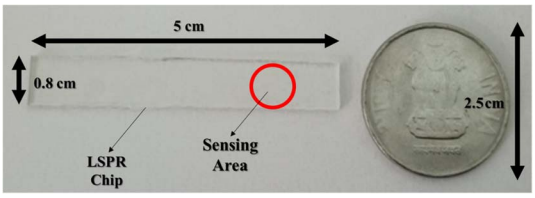

Fig. 1 Visual comparison illustrating the size of the fabricated LSPR chip in relation to an Indian currency coin.

2 Experimental methods

2.1 Chemicals and instruments

Bovine Serum Albumin (BSA), (3-aminopropyl)-triethoxysilane (≥98.0%) (APTES), maleic acid (MA), silver nitrate ($AgNO_3$), sodium hydroxide (NaOH), trisodium citrate (TSC), ammonium sulphate, salicylic acid, cyanuric acid and sodium borohydride ($NaBH_4$) was obtained from Merck, USA. Melamine (extra pure) and urea (extra pure) was procured from Loba Chemie. Hydrogen peroxide (30%) and formaldehyde (37%) were obtained from Emplura. Ethanol, acetone and methanol was procured from Qualigens and were utilised for cleaning. All glass wares and magnetic stirrers used in synthesis were dipped overnight in aqua regia and were later rinsed with distilled water (DW). The raw milk sample was purchased from a local vendor in Napaam, Tezpur-784028, Assam, India.

The optical characteristics of the NPs were recorded using a UV-vis spectrophotometer (Thermo Fisher GENESYS 180). Structural characteristics were recorded using X-ray powder diffractometer (Model: D8 FOCUS, Make: BRUKER AXS, Germany). Morphological aspects were studied using Field Emission Scanning Electron Microscope (FESEM) (Model: JSM-7200F, Make: JEOL), Transmission Electron Microscope (TEM) (TECNAI G2 20 S-TWIN (200KV) (Resolution: 2.4 Å, FEI Company, USA)) and Atomic Force Microscopy (AFM) (NTEGRA Vita device from NTMDT). Validation of the melamine content in spiked samples was performed by using High Performance Liquid Chromatography (HPLC) with UV/Vis Detection-2489 (HPLC Pump-515 Waters Corporation, USA). Additionally, other equipment such as a weighing machine (METTLER TOLEDO ME204), a centrifuge machine (Eppendorf 5430R), an oven (Echonian series; EQUITRON), and a magnetic stirrer (SPINOT-TARSONS) were utilized during the experimentation process.

2.2 Preparation silver nanoparticles (AgNPs)

28 mL of 2 mM $NaBH_4$ solution was combined with 12 mL of $AgNO_3$ solution, with continuous stirring over a 30 seconds interval. This resulted in synthesis of AgNPs depicted by a distinct colour change in the solution, transitioning from colourless to yellow. After this, the pH was adjusted to 7. For the functionalization of NPs, 2 mL of a 1 mM maleic acid solution was introduced to the NP solution, which was followed by stirring for about 10 min. Subsequently, the pH of the solution was brought to 7 by addition of NaOH (Fig. S1).[24]

2.3 Fabrication of plasmonic substrate

Microscopic glass slides were carefully cut into dimension measuring 0.8 cm in breadth and 5 cm in length using a glass cutter. These glass slides were then cleaned properly to ensure optimal surface conditions. For which, it was at first immersed in methanol, followed by sonication for 20 minutes, and then

Open Access Article. Published on 19 May 2026. Downloaded on 5/22/2026 8:11:50 PM. This article is licensed under a Creative Commons Attribution-NonCommercial 3.0 Unported Licence.

the slides were rinsed subsequently four times with DW to remove presence of any residual methanol on its surface. Following which, the substrate was immersed in 0.5% solution of APTES and heated at 50 °C for 1 hour. This step ensures effective functionalizing of the surface of glass slide for proper adhesion of the maleic acid functionalised AgNPs.[22]

After which the glass substrate was additionally rinsed with DW for five times to remove any residual unbounded APTES molecule on the surface of the glass slide. Finally, it was immersed in a solution of maleic acid-functionalised AgNPs for a period of 16 hours, allowing self-assembly of single layered NPs on the surface of glass slide.

Following the immobilization of NPs, the substrate was further washed with DW to remove any unbound NPs present on the glass surface. To block the surface of the glass slide from any non-specific interaction, the fabricated plasmonic chip was emersed in 1% solution of BSA for a period of 30 minutes. UV-vis measurements could not be reliably obtained in the absence of BSA, as the NPs without surface blocking were highly prone to aggregation and surface instability which may lead to false positive results (Fig. S2 and 2).[10,22,25]

2.4 Pre-treatment of milk

At first the milk was spiked with various concentration of melamine. After which, the spiked milk samples was pretreated using some simple steps to remove presence of unwanted fat and protien from it which may interfere with the detection process. Initially, 12 mL of 10% trichloroacetic acid was added to 40 mL of raw cow milk. The solution was then stirred using a glass rod and centrifuged for 15 minutes at 7000 rpm. After this, the milk supernatant was separated and transferred to a beaker, and the pH of the milk supernatant was adjusted to 7.0. Lastly, the milk supernatant was filtered through whatmann filter paper no. 1 and a 0.22-micron filter.[22,26]

In this procedure, trichloroacetic acid was added to the milk sample primarily to precipitate proteins and fats. During this acidic treatment, melamine present in the sample becomes protonated, forming soluble melaminium salt. In protonated form, melamine remains in the aqueous phase and does not co-precipitate with proteins or fats. After removal of the precipitated matrix components, the supernatant is carefully neutralized using NaOH. Upon neutralization, the melaminium ion is again deprotonated which converts it back to neutral melamine. Since melamine is relatively stable under these conditions and does not degrade during the acid–base treatment, it remains available for subsequent detection and quantification. This process ensures efficient removal of interfering milk components while retaining melamine in solution for accurate analysis.

2.5 Plasmonic sensing platform for detection of melamine

For sensing melamine, the fabricated LSPR chip is immersed in melamine spiked milk supernatant for half an hour, to allow the fabricated plasmonic substrate to interact with the melamine present on the milk supernatant samples. Following this step, the chip is ready for sensing. Using a standard UV-vis spectrophotometer, the chip is inserted into a cuvette along with the milk supernatant solution spiked with melamine. The UV-vis light emitted is directed onto the chip, and the detector records the transmitted light. A noticeable shift in the absorbance peak indicates the presence of melamine (Fig. 3).

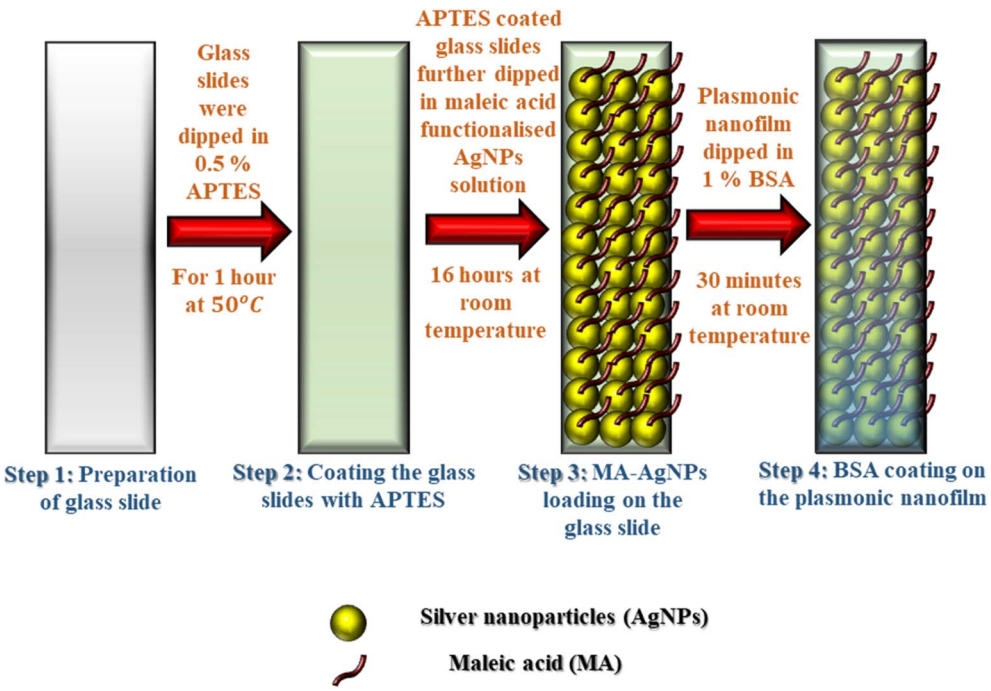

Fig. 2 Fabrication of plasmonically active glass chip.

© 2026 The Author(s). Published by the Royal Society of Chemistry

Open Access Article. Published on 19 May 2026. Downloaded on 5/22/2026 8:11:50 PM.
This article is licensed under a Creative Commons Attribution-NonCommercial 3.0 Unported Licence.

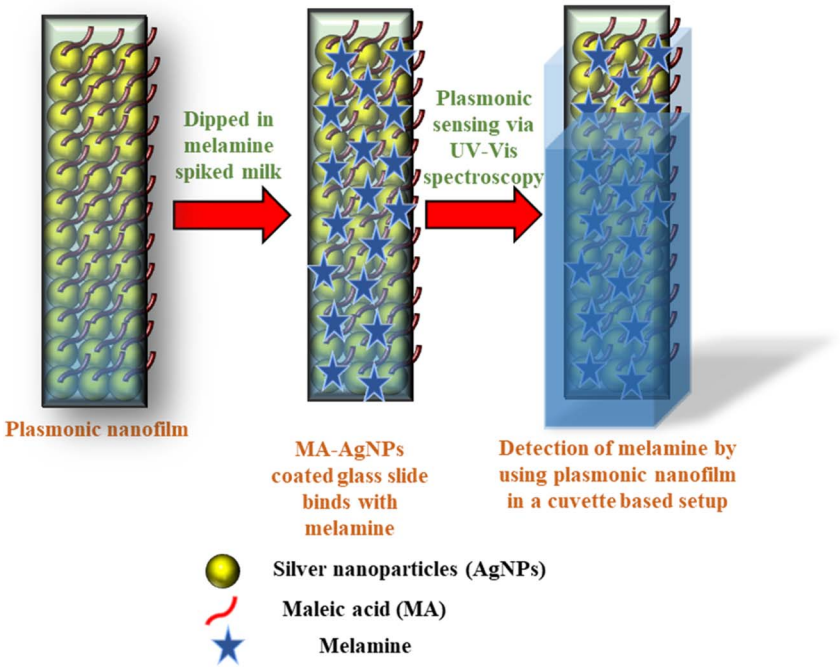

Fig. 3 Schematic representation of plasmonic sensing of melamine in milk by LSPR chip.

3 Results and discussion

3.1 Characterisation of the maleic acid functionalised silver nanoparticles

3.1.1 Optical study. UV-vis spectroscopy study was performed to study the absorption spectra of the synthesised MA-AgNPs. Distinct absorbance spectrum was obtained in the visible region between 350 nm to 700 nm (Fig. 4). An intense absorbance peak was obtained at 408 nm which is the LSPR peak of the synthesised MA-AgNPs. This peak arises due to resonance, which occurs when the conduction electrons in a metal NP, undergoes collective oscillations in response to incident electromagnetic radiation. This collective oscillation is responsible for strong absorption of incoming light at a specific wavelength known as resonance wavelength.[27]

3.1.2 Structural study. The XRD data was obtained within the 2θ range between 35 to 80°. Four distinct diffraction peaks were observed, which depicted crystalline nature of the synthesized AgNPs. Diffraction peaks were obtained at 37.54°, 43.72°, 63.98°, and 76.96°, corresponding to the (111), (200),

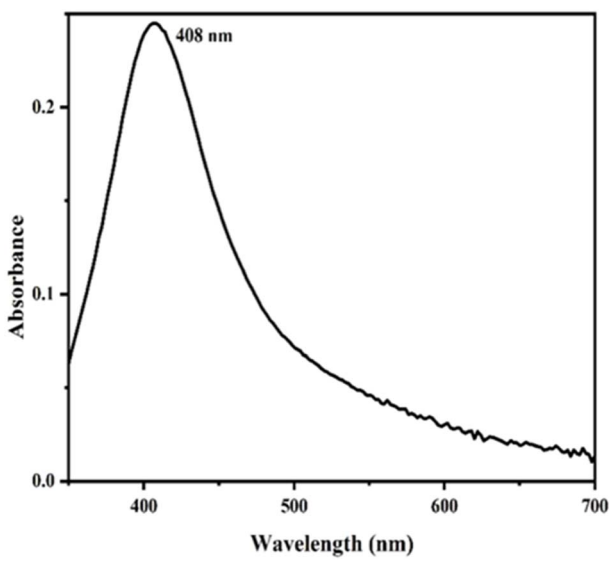

Fig. 4 Optical characterisation of MA-AgNPs by UV-vis spectrophotometer.

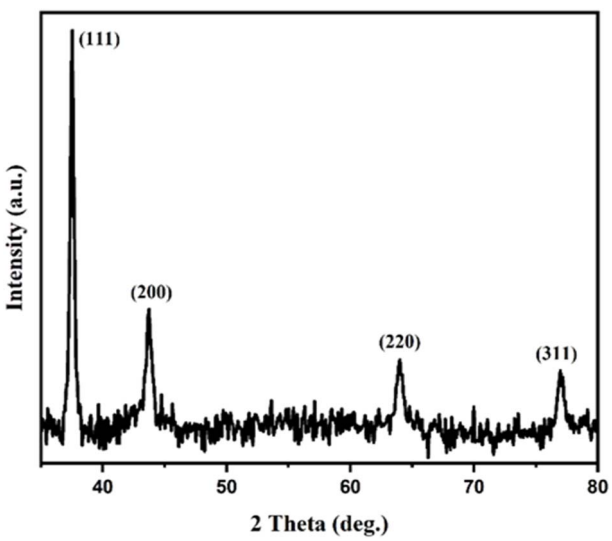

Fig. 5 Structural characterisation of MA-AgNPs by XRD.

Open Access Article. Published on 19 May 2026. Downloaded on 5/22/2026 8:11:50 PM.
This article is licensed under a Creative Commons Attribution-NonCommercial 3.0 Unported Licence.

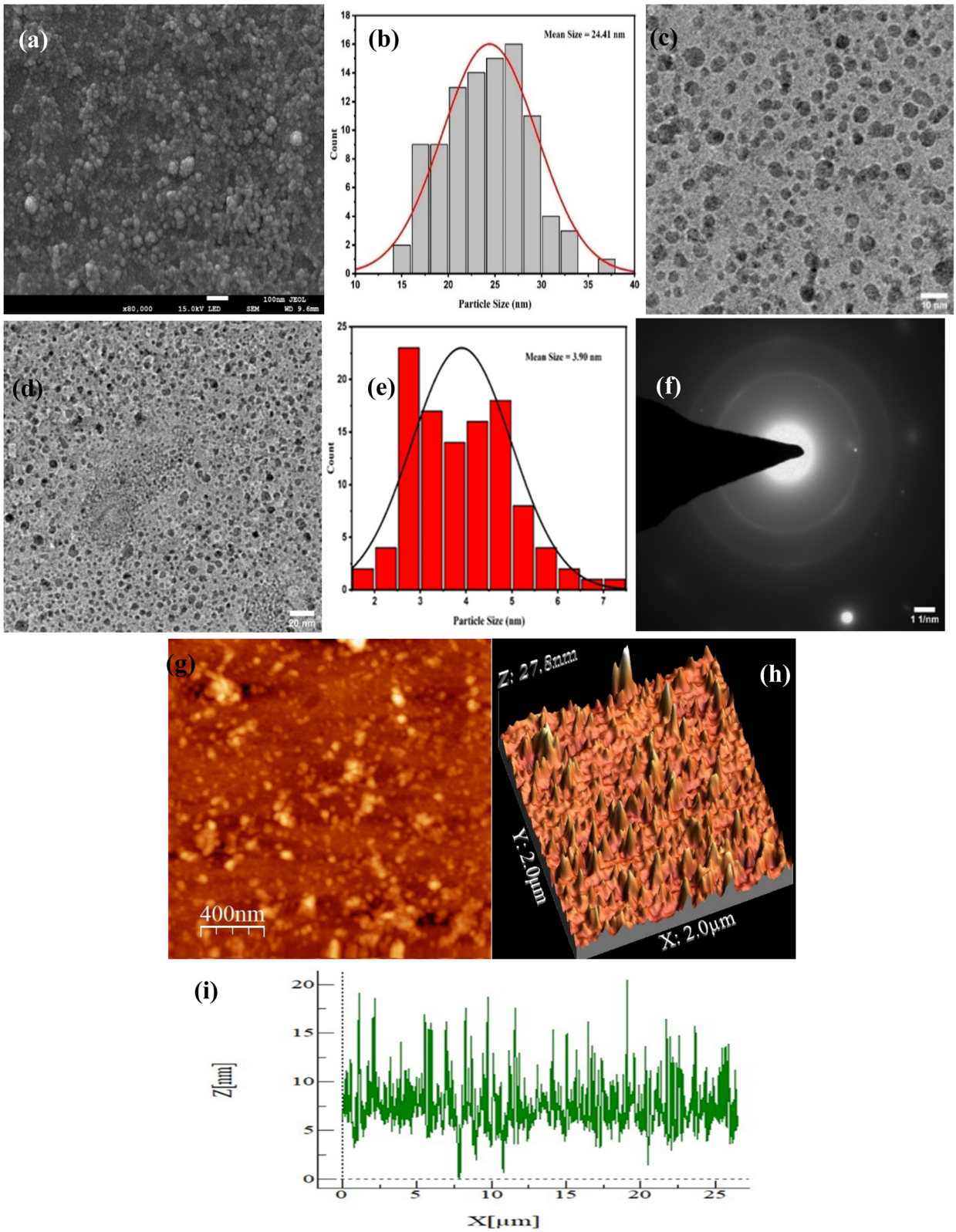

Fig. 6 Morphology and surface characterization of MA-AgNPs from: FESEM study (a) FESEM image, (b) distribution of diameter of NPs; TEM study (c) highly magnified TEM image, (d) TEM image, (e) distribution of diameter of NPs, (f) SAED pattern; AFM study (g) 2D view, (h) 3D view, and (i) height distribution profile of NPs on the surface of glass chip.

© 2026 The Author(s). Published by the Royal Society of Chemistry

Open Access Article. Published on 19 May 2026. Downloaded on 5/22/2026 8:11:50 PM. This article is licensed under a Creative Commons Attribution-NonCommercial 3.0 Unported Licence.

(220), and (311) planes of Ag. Each peak has been labelled accordingly in (Fig. 5). The most intense peak was observed at an angle of 37.54°, indicating the preferential orientation of the (111) crystallographic plane. The presence of these characteristic diffraction peaks confirms that the synthesized AgNPs exhibits a face centred cubic (FCC) crystalline structure.[28]

3.1.3 Morphological study

3.1.3.1 Field emission scanning electron microscopy. FESEM analysis was performed to determine the morphological characteristics of the synthesized AgNPs. For this, the fabricated LSPR sensor was cut into dimensions of 0.5 cm × 0.5 cm and spin-coated. The FESEM images revealed that the NPs exhibited a spherical morphology. The mean diameter of these NPs was approximately 24 nm, with individual particle sizes ranging from 12 to 38 nm (Fig. 6a and b).[29] The larger apparent size in FESEM is attributed to overestimation caused by surface aggregation and environmental effects when NPs are immobilized on the glass substrate.

3.1.3.2 Transmission electron microscopy. TEM analysis was performed by sonicating the synthesized AgNPs in liquid media, followed by drop-casting onto a copper grid and vacuum drying at room temperature. The size distribution analysis from TEM images showed much smaller NPs, ranging from 1 to 10 nm, with an average diameter of approximately 4 nm (Fig. 6c–f). The TEM images confirmed the spherical morphology of individual NPs. The smaller size observed in TEM is due to imaging of well-dispersed, individual NPs in liquid media, minimizing aggregation compared to FESEM.[29,30]

3.1.3.3 Atomic force microscopy. The analysis was conducted following a protocol similar to that employed for FESEM analysis, at first the glass slides were cut into dimensions of 1 cm × 1 cm. The images obtained from the AFM study displayed homogeneous distribution of MA-AgNPs onto the glass slide, which can be observed in both 2D and 3D representations of the AFM images. From the AFM image a surface profile analysis was performed to ascertain the distribution of height of the NP on the surface of glass slide, which was found to be between 5 to 20 nm. This range closely aligns with the size of the synthesized NPs as confirmed by TEM and FESEM studies. This suggests that the glass slides were coated with a thin, single-layered NP coating (Fig. 6g–i).[18,31,32]

3.2 Sensing mechanism

The maleic acid compound, contains two carboxylic groups, it is a bis-carboxylic acid derivative which exhibits a unique structural configuration and can be easily bounded onto the surface of bare NPs. Its interaction with melamine, which is rich in amine groups, is orchestrated by hydrogen bonding. Specifically, the hydrogen of the amine group in melamine forms bonds with the maleic acid attached to the NP surface. This hydrogen bonding involves the oxygen atom of the maleic acid group interacting with the hydrogen atom of the amine group in melamine (Fig. 7). This interaction is responsible for changes in the refractive index of the surrounding medium which brings about a shift in the plasmonic peak position. Here, BSA acts as a blocking agent to prevent adsorption of other milk components onto the surface of MA-AgNP during melamine detection.

To perform sensing, the maleic acid (MA)-functionalized AgNPs were immobilized onto a glass substrate using APTES (3-aminopropyltriethoxysilane) which acts as an adhesive and facilitates binding of functionalised NPs on the surface of glass slide. Upon exposure to a milk solution containing melamine, the surface functionalization helps in interactions with the three amine groups of melamine, resulting in a discernible red shift in the plasmonic peak as a result of shift in refractive index due to external bindings.[10,22] However, as melamine possess a triazine ring structure containing multiple amine groups, which enables binding of the NH_2 group with the carboxyl groups of maleic acid. This results in a distinct and more

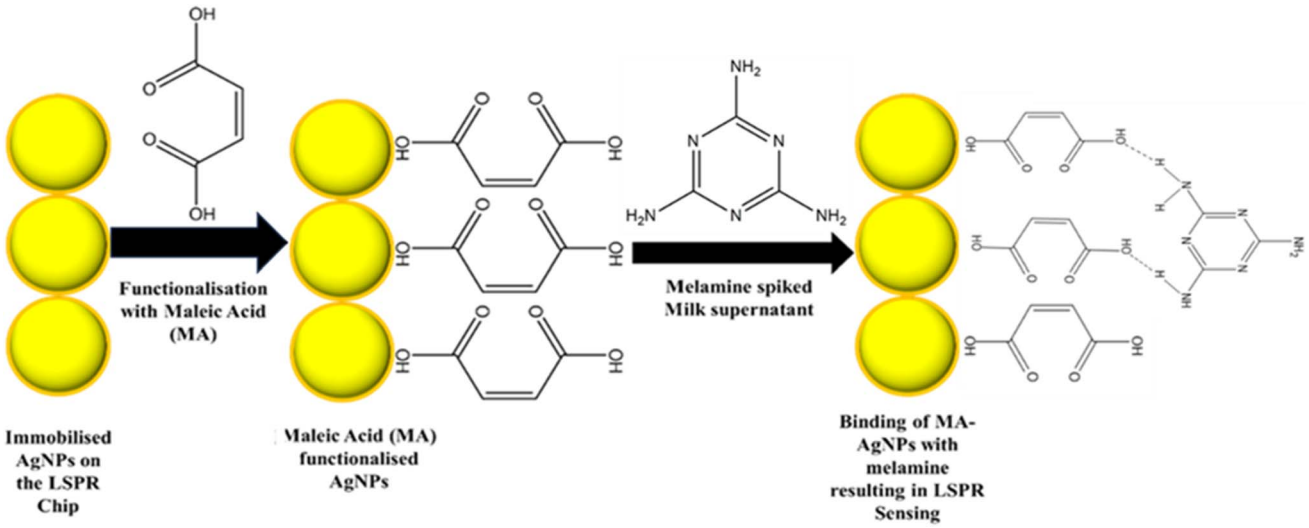

Fig. 7 Schematic illustration representing working principle of the fabricated plasmonic chip.

Open Access Article. Published on 19 May 2026. Downloaded on 5/22/2026 8:11:50 PM.
This article is licensed under a Creative Commons Attribution-NonCommercial 3.0 Unported Licence.

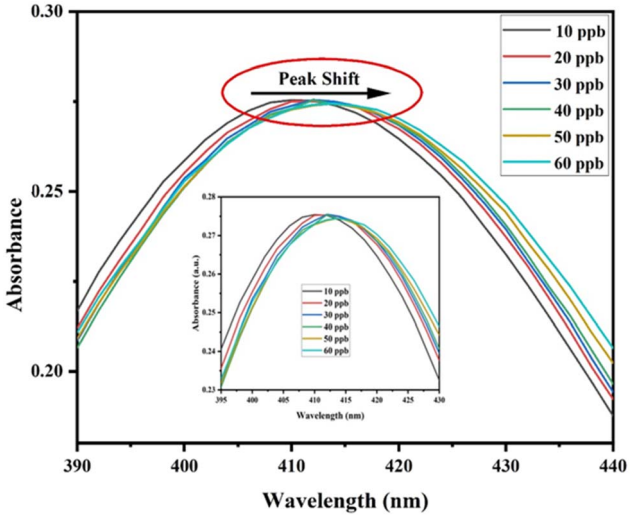

Fig. 8 UV-vis spectra depicting peak shift with increase in melamine concentration in milk.

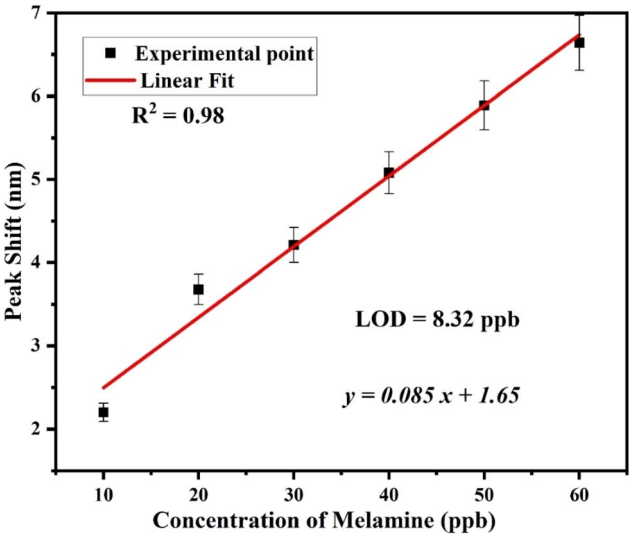

Fig. 9 Linear calibration graph between peak shift and melamine concentration in milk.

pronounced LSPR shift compared to that caused by other simple mono- or diamine compounds. Additionally, the sensing study has been designed for controlled aqueous and milk system, where melamine is the primary target analyte. In such environments, common biological amines are either absent or present in very low concentrations after sample preparation, minimizing any interference.

3.3 Sensor performance metrics

As the concentration of melamine increased, a clear shift in the plasmonic peak was observed in the UV-vis spectra (Fig. 8), demonstrating the feasibility of using this system for quantitative detection. A linear correlation was established between the peak shift and melamine concentration, which was used to plot a calibration graph. The limit of detection (LOD) was determined to be 8.32 ppb, calculated using the standard formula:

$$\mathrm{LOD} = \frac{3.3\sigma}{s}$$

where σ is the standard deviation of blank measurements ($n = 3$) and s is the slope of the calibration curve. The sensor exhibited a dynamic range from 10 to 60 ppb, confirming its ability to detect melamine at trace concentrations. The sensitivity of the plasmonic system was 0.085 nm ppb^{-1}, indicating that even small changes in melamine concentration can be reliably detected (Fig. 9).[10,22,33] The recovery of the sensor, assessed *via* spiked samples, ranged from 94% to 104%, highlighting its accuracy. For practical demonstration, the system was applied to detect trace melamine in milk. Unknown milk samples were spiked with melamine, and the experimental errors were found to be 0.4–6%, confirming that the plasmonic sensor provides reliable quantitative results.[6,33,34]

In this procedure, the peak shift was first measured for each sample. The experimental melamine concentration was then obtained from the linear calibration graph, and compared with the theoretical value to calculate the error (Table 1). While the setup is a proof-of-concept, these results demonstrate that the proposed plasmonic sensing strategy is robust, sensitive, and suitable for trace-level melamine detection.

3.4 Interference study

Furthermore, selective analysis was performed to evaluate the susceptibility of the detection process due to interference from other adulterants, using UV-vis method. To perform the selectivity study 10 ppb concentration of melamine was used whereas 100 ppb of other adulterants were spiked to milk

Table 1 Quantitative estimation of amount of melamine in milk supernatant as determined by the LSPR method

Sl. no.	Shift in plasmonic peak (y) (nm)	Theoretical concentration of melamine (x_0) (ppb)	Experimental concentration of melamine (x) (ppb)	Percentage of error $\left\lvert\frac{x_0 - x}{x_0}\right\rvert \times 100\%$
1	2.092	5	5.2	4
2	2.917	15	14.9	0.6
3	3.648	25	23.5	6
4	4.727	35	36.2	3.4
5	5.458	45	44.8	0.4

© 2026 The Author(s). Published by the Royal Society of Chemistry

Open Access Article. Published on 19 May 2026. Downloaded on 5/22/2026 8:11:50 PM.
This article is licensed under a Creative Commons Attribution-NonCommercial 3.0 Unported Licence.

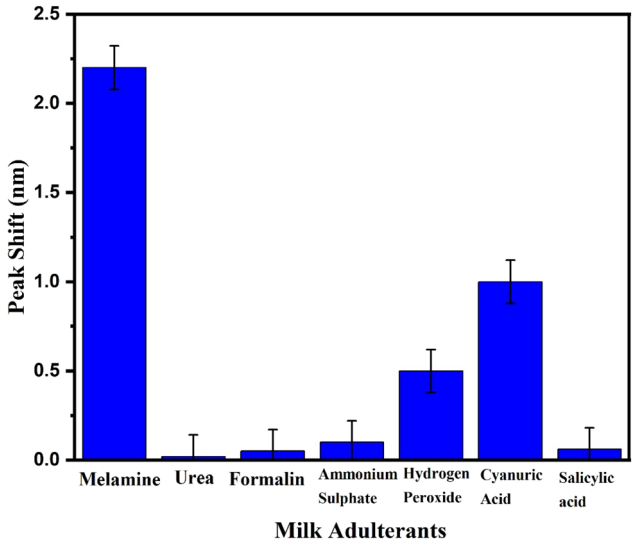

Fig. 10 Selectivity analysis of the LSPR chip towards detection of melamine.

samples. It was found that only presence of melamine resulted in significant shift in absorbance peak compared to the other adulterants added to milk. But a small amount of peak shift was also observed in case of cyanuric acid as its chemical structure is quite similar to milk adulterant melamine. But this interference was only observed for higher concentration of cyanuric acid in milk compared to that of melamine which displayed significant shift in plasmonic peak even at low concentration (Fig. 10).

3.5 Comparative analysis with previously reported works

Colorimetric methods are often employed as a qualitative tool for sensing of adulterants in milk. However, various other methods are also reported in the literature which could be used to ensure accurate assessment of the adulterant melamine, but most of them provide a qualitative solution for its detection and also are unable to detect trace amount of adulterant melamine in milk. To solve this problem a more precise inexpensive technique is required which is capable of detecting melamine even at trace amounts. This level of sensitivity can only be achieved using LSPR-based plasmonic nanofilms. These nanofilms detect subtle changes in the refractive index of the medium surrounding the NPs, enabling selective and precise quantification of melamine.

While previous studies reported in literature,[35] where some are listed in (Table 2)—have reported lower LOD, our work distinguishes itself through its use of LSPR-based plasmonic nanofilms, which provides a unique combination of label-free sensing, real-time monitoring, with high specificity. Unlike conventional colorimetric methods that are primarily qualitative and often lack the sensitivity to detect trace levels of adulterants, our approach leverages changes in the local refractive index around plasmonic NPs to achieve selective and accurate quantification. This makes this method especially advantageous for practical on-site applications where reliability, reproducibility, and minimal sample preparation are essential. Moreover, the cost of fabrication of the nanofilms in our method is also quite low and is simple compared to the other reported works. Therefore, even when compared with studies reporting lower LODs, the novelty of our method lies in its integration of precision, ease of deployment, and adaptability for real-world milk quality monitoring.

Table 2 Comparative study of melamine sensing in milk by plasmonic NPs as reported in literature

Sensing system	Recovery	Lowest limit of sensing/LOD	Reference
Trisodium citrate-AuNPs	95–105%	0.05 ppm	36
1-(2-Mercaptoethyl)-1,3,5-triazinane-2,4,6-trione (MTT)-AuNPs	—	2.5 ppb	37
Trisodium citrate-AgNPs	88.83–114.29%	0.29 ppm	38
Sulfanilic acid-AgNPs	103–109%	1.34 ppb	39
Ascorbic Acid-AgNPs	—	100 ppb	34
Chitosan/tripolyphosphate-AuNPs	85–107%	6 ppb	40
Gallic acid-AgNPs	97.1–102.6%	0.456 ppb	41
β-cyclodextrin-AgNPs	80.5–109.02%	0.628 ppm	17
p-Nitroaniline (p-NA)-AgNPs	—	100 ppb	42
Dopamine-AgNPs	98.5%	10 ppb	43
Jotropha gossypifolia-AgNPs	96–122%	252 ppb	44
Tannic acid-AgNPs	99.5–106.5%	1.26 ppb	19
Parthenium histerophorus-AgNPs	96%	0.5 ppm	45
Green tea-AgNPs	93%	1.44 ppm	6
p-NA-AuNPs (cuvette based)	—	0.01 ppb	10
Trisodium citrate-AuNPs (optical fibre based)	99.2–111%	4.16 ppb	46
Glassy carbon electrode (GCE) modified with copper nanoflowers (NFs) with reduced graphene oxide (r-GO)	87.76–90.43%	0.63 ppb	47
MA-AgNPs (cuvette based)	**94%–104%**	**8.32 ppb**	**Reported work**

Open Access Article. Published on 19 May 2026. Downloaded on 5/22/2026 8:11:50 PM. This article is licensed under a Creative Commons Attribution-NonCommercial 3.0 Unported Licence.

4 Conclusion

The study reports quantitative estimation of trace amount of melamine in milk by using plasmonic nanofilm based LSPR chip. Through a comprehensive characterization technique, the optical, structural and morphological properties of the synthesized maleic acid functionalised AgNPs was studied. These functionalized MA-AgNPs, displayed strong interaction towards melamine, resulting in a notable shift in the absorbance peak. Moreover, the plasmonic activity of the LSPR chip was also evaluated by determining the selectivity, sensitivity, dynamic range of sensing, and recovery efficiency of the sensing platform towards melamine detection. Additionally, validation experiments were also performed using HPLC technique which further corroborated the sensor's accuracy and precision in detecting melamine in milk (SI Material 1) (Fig. S3). The innovative design of the chip, leverages the LSPR technology and demonstrates high sensitivity along with high reproducibility with a LOD of 8.32 ppb. The results not only contribute to advancing on-site detection technologies but also emphasize the LSPR chip's potential for broader applications in ensuring food safety.

Author contributions

UD: conceptualization, data curation, formal analysis, writing original draft. TD: data curation, methodology. RB: project administration, supervision, writing and reviewing. NM: reviewing draft.

Conflicts of interest

The authors declare no conflicts of interest.

Data availability

All the data associated with the study are already added to the manuscript.

Supplementary information (SI) is available. See DOI: https://doi.org/10.1039/d5ra05664k.

Acknowledgements

Author UD would like to gratefully acknowledge the Department of Science and Technology, Government of India for providing financial assistance in form of DST INSPIRE Fellowship [DST/INSPIRE Fellowship/2019/IF190914]. Authors would also like to acknowledge, Sophisticated Analytical Instrumentation Centre (SAIC), Tezpur university and SAIC, Institute of Advanced Study in Science and Technology, Guwahati (IASST) for providing the instrumentation facilities. Authors would also like to thank Department of Biotechnology (DBT) and the Biotechnology Industry Research Assistance Council (BIRAC) for providing the UV-vis spectroscopy facility. Research support received from DST-FIST and UGC-SAP DRS II grant in aid to the Department of Physics is also gratefully acknowledged.

References

1 L. Wang, M. Hasanzadeh Kafshgari and M. Meunier, Optical properties and applications of plasmonic-metal NPs, *Adv. Funct. Mater.*, 2020, **30**(51), 2005400, DOI: 10.1002/adfm.202005400.
2 S. B. Borah, T. Bora, S. Baruah and J. Dutta, Heavy metal ion sensing in water using surface plasmon resonance of metallic nanostructures, *Groundw. Sustain. Dev.*, 2015, **1**(1–2), 1–11, DOI: 10.1016/j.gsd.2015.12.004.
3 N. M. Dissanayake, J. S. Arachchilage, T. A. Samuels and S. O. Obare, Highly sensitive plasmonic metal nanoparticle-based sensors for the detection of organophosphorus pesticides, *Talanta*, 2019, **200**, 218–227, DOI: 10.1016/j.talanta.2019.03.042.
4 U. Das, R. Hoque and R. Biswas, Biosynthesised AgNPs as an efficient colorimetric sensor towards detection of melamine, *Appl. Phys. A Mater.*, 2023, **129**(5), 328, DOI: 10.1007/s00339-023-06613-1.
5 J. Choi, J. H. Kim, J. W. Oh and J. M. Nam, Surface-enhanced Raman scattering-based detection of hazardous chemicals in various phases and matrices with plasmonic nanostructures, *Nanoscale*, 2019, **11**(43), 20379–20391, DOI: 10.1039/C9NR07439B.
6 U. Das, R. Biswas and N. Mazumder, One-pot interference-based colorimetric detection of melamine in raw milk *via* green tea-modified Ag nanostructures, *ACS Omega*, 2024, **9**(20), 21879–21890, DOI: 10.1021/acsomega.3c09516.
7 X. Pei, A. Tandon, A. Alldrick, L. Giorgi, W. Huang and R. Yang, The China melamine milk scandal and its implications for food safety regulation, *Food Policy*, 2011, **36**(3), 412–420, DOI: 10.1016/j.foodpol.2011.03.008.
8 Q. Li, P. Song and J. Wen, Melamine and food safety: a 10-year review, *Curr. Opin. Food Sci.*, 2019, **30**, 79–84, DOI: 10.1016/j.cofs.2019.05.008.
9 N. Kumar, *Development of a Simple Colorimetric Method for Detection of Melamine in Milk Using Nantechnology, PhD Dissertation*, NDRI, 2014.
10 S. Y. Oh, M. J. Lee, N. S. Heo, S. Kim, J. S. Oh, Y. Lee and Y. S. Huh, Cuvette-type LSPR sensor for highly sensitive detection of melamine in infant formulas, *Sensors*, 2019, **19**(18), 3839, DOI: 10.3390/s19183839.
11 Y. Liu, E. E. Todd, Q. Zhang, J. R. Shi and X. J. Liu, Recent developments in the detection of melamine, *J. Zhejiang Univ., Sci., B*, 2012, **13**(7), 525–532, DOI: 10.1631/jzus.B1100389.
12 P. Lutter, M. C. Savoy-Perroud, E. Campos-Gimenez, L. Meyer, T. Goldmann, M. C. Bertholet and T. Delatour, Screening and confirmatory methods for the determination of melamine in cow's milk and milk-based powdered infant formula: Validation and proficiency-tests of ELISA, HPLC-UV, GC-MS and LC-MS/MS, *Food Control*, 2011, **22**(6), 903–913, DOI: 10.1016/j.foodcont.2010.11.022.
13 Y. Qiu, Y. Tang, B. Li, C. Gu and M. He, Aptamer-based detection of melamine in milk using an evanescent wave

© 2026 The Author(s). Published by the Royal Society of Chemistry

Open Access Article. Published on 19 May 2026. Downloaded on 5/22/2026 8:11:50 PM. This article is licensed under a Creative Commons Attribution-NonCommercial 3.0 Unported Licence.

fiber sensor, *Anal. Methods*, 2018, **10**(40), 4871–4878, DOI: 10.1039/C8AY01594E.
14 S. Singh, V. Kaur, N. Kumar, M. Garg, S. K. Pandey and V. K. Meena, Cadmium chalcogenide derived fluorescent quanta-sensor for melamine detection, *Sens. Actuators, B Chem.*, 2018, **273**, 505–510, DOI: 10.1016/j.snb.2018.06.063.
15 I. E. Paul, A. Rajeshwari, T. C. Prathna, A. M. Raichur, N. Chandrasekaran and A. Mukherjee, Colorimetric detection of melamine based on the size effect of AuNPs, *Anal. Methods*, 2015, **7**(4), 1453–1462, DOI: 10.1039/C4AY02622E.
16 Z. Wu, H. Zhao, Y. Xue, Q. Cao, J. Yang, Y. He and Z. Yuan, Colorimetric detection of melamine during the formation of gold NPs, *Biosens. Bioelectron.*, 2011, **26**(5), 2574–2578, DOI: 10.1016/j.bios.2010.11.007.
17 S. S. J. Xavier, C. Karthikeyan, A. R. Kim and D. J. Yoo, Colorimetric detection of melamine using β-cyclodextrin-functionalized AgNPs, *Anal. Methods*, 2014, **6**(20), 8165–8172, DOI: 10.1039/C4AY01183J.
18 W. Chen, H. H. Deng, L. Hong, Z. Q. Wu, S. Wang, A. L. Liu and X. H. Xia, Bare gold NPs as facile and sensitive colorimetric probe for melamine detection, *Analyst*, 2012, **137**(22), 5382–5386, DOI: 10.1039/C2AN35962F.
19 M. F. Alam, A. A. Laskar, S. Ahmed, M. A. Shaida and H. Younus, Colorimetric method for the detection of melamine using in-situ formed AgNPs *via* tannic acid, *Spectrochim. Acta, Part A*, 2017, **183**, 17–22, DOI: 10.1016/j.saa.2017.04.021.
20 S. Liu, A. Kannegulla, X. Kong, R. Sun, Y. Liu, R. Wang and A. X. Wang, Simultaneous colorimetric and surface-enhanced Raman scattering detection of melamine from milk, *Spectrochim. Acta, Part A*, 2020, **231**, 118130, DOI: 10.1016/j.saa.2020.118130.
21 J. Xue, P. T. Lee and R. G. Compton, Electrochemical detection of melamine, *Electroanalysis*, 2014, **26**(7), 1454–1460, DOI: 10.1002/elan.201400166.
22 U. Das, R. Biswas and N. Mazumder, Quantifying Hydrogen Peroxide in Cattle Milk *via* a Novel Plasmonic Nanofilm, *ACS Omega*, 2025, **10**(21), 21786–21794, DOI: 10.1021/acsomega.5c01585.
23 U. Das, S. Saikia and R. Biswas, Highly sensitive biofunctionalized nanostructures for paper-based colorimetric sensing of hydrogen peroxide in raw milk, *Spectrochim. Acta, Part A*, 2024, **316**, 124290, DOI: 10.1016/j.saa.2024.124290.
24 K. Ramalingam, T. Devasena, B. Senthil, R. Kalpana and R. Jayavel, AgNPs for melamine detection in milk based on transmitted light intensity, *IET Sci., Meas. Technol.*, 2017, **11**(2), 171–178, DOI: 10.1049/iet-smt.2016.0215.
25 S. Y. Oh, N. S. Heo, V. K. Bajpai, S. C. Jang, G. Ok, Y. Cho and Y. S. Huh, Development of a cuvette-based LSPR sensor chip using a plasmonically active transparent strip, *Front. Bioeng. Biotechnol.*, 2019, **7**, 299, DOI: 10.3389/fbioe.2019.00299.
26 W. Xie, Y. Huang, W. Yun, D. Tang, H. Zhang, C. Du and W. Zhang, Simple Pretreatment and Portable UV-Vis Spectrum Instrument for the Rapid Detection of Melamine in Milk Products, *J. Food Qual.*, 2015, **38**(4), 297–304, DOI: 10.1111/jfq.12146.
27 G. Moreno-Martin, M. E. León-González and Y. Madrid, Simultaneous determination of the size and concentration of AgNPs in water samples by UV–vis spectrophotometry and chemometrics tools, *Talanta*, 2018, **188**, 393–403, DOI: 10.1016/j.talanta.2018.06.009.
28 S. S. Abdulsahib, Synthesis, characterization and biomedical applications of AgNPs, *Biomedicine*, 2021, **41**(2), 458–464.
29 M. E. Taghavizadeh Yazdi, J. Khara, M. R. Housaindokht, H. R. Sadeghnia, S. Esmaeilzadeh Bahabadi, M. Sadegh Amiri and M. Darroudi, Role of Ribes khorassanicum in the biosynthesis of AgNPs and their antibacterial properties, *IET Nanobiotechnol.*, 2019, **13**(2), 189–192, DOI: 10.1049/iet-nbt.2018.5215.
30 P. Verma and S. K. Maheshwari, Preparation of sliver and selenium NPs and its characterization by dynamic light scattering and scanning electron microscopy, *J. Microsc. Ultrastruct.*, 2018, **6**(4), 182–187, DOI: 10.4103/JMAU.JMAU_3_18.
31 J. Zhu, Y. Tian, L. Cao, J. Hu, J. Yan, Z. Wang and X. Liu, Comparison of the effects of AgNPs on the morphological and mechanical characteristics of cancerous cells, *J. Microsc.*, 2023, **289**(3), 187–197, DOI: 10.1111/jmi.13166.
32 I. Horcas, R. Fernández, J. M. Gomez-Rodriguez, J. Colchero, J. Gómez-Herrero and A. M. Baro, WSXM: A software for scanning probe microscopy and a tool for nanotechnology, *Rev. Sci. Instrum.*, 2007, **78**(1), 013705, DOI: 10.1063/1.2432410.
33 X. Liu, J. Wang, Y. Wang, C. Huang, Z. Wang and L. Liu, In situ functionalization of AgNPs by gallic acid as a colorimetric sensor for simple sensitive determination of melamine in milk, *ACS Omega*, 2021, **6**(36), 23630–23635, DOI: 10.1021/acsomega.1c03927.
34 S. Varun, S. K. Daniel and S. S. Gorthi, Rapid sensing of melamine in milk by interference green synthesis of AgNPs, *Mater. Sci. Eng., C*, 2017, **74**, 253–258, DOI: 10.1016/j.msec.2016.12.011.
35 U. Das and R. Biswas, Advances in Plasmonic Nanoprobes for sensitive detection of key Milk adulterants: A comprehensive review, *Microchem. J.*, 2025, **218**, 115543, DOI: 10.1016/j.microc.2025.115543.
36 N. Kumar, R. Seth and H. Kumar, Colorimetric detection of melamine in milk by citrate-stabilized gold NPs, *Anal. Biochem.*, 2014, **456**, 43–49, DOI: 10.1016/j.ab.2014.04.002.
37 K. Ai, Y. Liu and L. Lu, Hydrogen-bonding recognition-induced color change of gold NPs for visual detection of melamine in raw milk and infant formula, *J. Am. Chem. Soc.*, 2009, **131**(27), 9496–9497, DOI: 10.1021/ja9037017.
38 H. Ping, M. Zhang, H. Li, S. Li, Q. Chen, C. Sun and T. Zhang, Visual detection of melamine in raw milk by label-free AgNPs, *Food Control*, 2012, **23**(1), 191–197, DOI: 10.1016/j.foodcont.2011.07.009.
39 J. Song, F. Wu, Y. Wan and L. Ma, Colorimetric detection of melamine in pretreated milk using AgNPs functionalized with sulfanilic acid, *Food Control*, 2015, **50**, 356–361, DOI: 10.1016/j.foodcont.2014.08.049.

Open Access Article. Published on 19 May 2026. Downloaded on 5/22/2026 8:11:50 PM.
This article is licensed under a Creative Commons Attribution-NonCommercial 3.0 Unported Licence.

40 H. Guan, J. Yu and D. Chi, Label-free colorimetric sensing of melamine based on chitosan-stabilized gold NPs probes, *Food Control*, 2013, **32**(1), 35–41, DOI: 10.1016/j.foodcont.2012.11.041.

41 M. Farrokhnia, S. Karimi and S. Askarian, Strong hydrogen bonding of gallic acid during synthesis of an efficient AgNPs colorimetric sensor for melamine detection *via* dis-synthesis strategy, *ACS Sustain. Chem. Eng.*, 2019, **7**(7), 6672–6684, DOI: 10.1021/acssuschemeng.8b05785.

42 C. Han and H. Li, Visual detection of melamine in infant formula at 0.1 ppm level based on AgNPs, *Analyst*, 2020, **135**(3), 583–588, DOI: 10.1039/B923424A.

43 Y. Ma, H. Niu, X. Zhang and Y. Cai, One-step synthesis of silver/dopamine nanoparticles and visual detection of melamine in raw milk, *Analyst*, 2011, **136**(20), 4192–4196, DOI: 10.1039/c1an15327g.

44 H. P. Borase, C. D. Patil, R. B. Salunkhe, R. K. Suryawanshi, B. K. Salunke and S. V. Patil, Biofunctionalized AgNPs as a novel colorimetric probe for melamine detection in raw milk, *Biotechnol. Appl. Biochem.*, 2015, **62**(5), 652–662, DOI: 10.1002/bab.1306.

45 S. K. Daniel, L. A. N. Julius and S. S. Gorthi, Instantaneous detection of melamine by interference biosynthesis of AgNPs, *Sens. Actuators, B*, 2017, **238**, 641–650, DOI: 10.1016/j.snb.2016.07.112.

46 K. Chang, S. Wang, H. Zhang, Q. Guo, X. Hu, Z. Lin and J. Hu, Colorimetric detection of melamine in milk by using gold NPs-based LSPR *via* optical fibers, *PLoS One*, 2017, **12**(5), e0177131, DOI: 10.1371/journal.pone.0177131.

47 M. Daizy, C. Tarafder, M. R. Al-Mamun, X. Liu, M. Aly Saad Aly and M. Z. H. Khan, Electrochemical detection of melamine by using reduced graphene oxide–copper nanoflowers modified glassy carbon electrode, *ACS Omega*, 2019, **4**(23), 20324–20329, DOI: 10.1021/acsomega.9b02827.

© 2026 The Author(s). Published by the Royal Society of Chemistry